Effect of particles on the induction time of calcium carbonate in synthetic SWRO concentrate

Tarek Waly[a,b,]*, Ruben Munoz[a], Maria D. Kennedy[a], Geert Jan Witkamp[b], Gary Amy[a,b], Jan C. Schippers[a]

[a]*UNESCO-IHE, Institute for Water Education, Westvest 7, 2611 AX Delft, The Netherlands*
[b]*Delft University of Technology, Stevinweg 1, 2628 CN Delft, The Netherlands*
Tel.: +31 15 2151715; email: t.waly@unesco-ihe.org

ABSTRACT

Particles, which are naturally present in seawater, have been reported to affect the formation of $CaCO_3$ crystals. In this study the effect of foreign particles on induction time was explored. Induction time was monitored using a highly sensitive pH meter mounted in an air-tight glass reactor. Experimental work was performed with synthetic seawater prepared using ultra-pure water with a composition equivalent to 50% recovery SWRO concentrate (based on the composition of seawater from the Gulf of Oman). The prepared synthetic solutions were filtered through filters having different pore sizes namely 0.22 μm; 0. μm and 100kD (≈0.03 μm). In addition, glass beads of diameter 20–30 nm were added in volumes of (1; 0.5 and 0.1 ml) to synthetic seawater to yield an increase in glass/water contact area of 123%, 16% and 1% compared to the total reactor glass area in contact with the synthetic water. Different mixing speeds were applied namely 10; 50; 150 and 300 rpm to investigate the effect of mixing on experimental results. Results showed that filtering synthetic seawater and applying different mixing speeds had a negligible effect on the experimental induction time results. On the contrary, the addition of glass beads shortened the induction time substantially from 30% to 100% (immediate precipitation), depending on the amount of beads added.

Keywords: Induction time; Membrane; Calcium carbonate; Glass beads; Filtration

1. Introduction

Reducing the consumption of chemicals in seawater reverse osmosis (SWRO) plants is an important goal because of the positive impact on the environment and the reduction in operational costs. Acid/antiscalant dosing to avoid calcium carbonate scale is responsible for a major part of the chemical consumption in SWRO. Reducing chemical dosing can be achieved by determining the actual scaling limits of calcium carbonate in SWRO, and operating close to these limits. This can be achieved by investigating the factors affecting the nucleation mechanism of $CaCO_3$ in seawater concentrates.

Particles generally exist in natural aquatic environments and seawater is no exception to this rule. Indeed, these particles might be different in terms of their nature, size and concentration, but generally they can be classified as: settleable solids (>100 μm), supra-colloidal solids (1 μm to 100 μm), colloidal solids (0.001 μm to 1μm) and dissolved solids (<0.001 μm) [1]. The most common inorganic colloids in natural waters are aluminum silicate clays and colloids of iron, aluminum and silica. Organic deposits, together with iron oxide, silica

*Corresponding author.

and aluminum, represent 70% of the deposits detected in membrane autopsies throughout the world [2,3]. Natural seawater contains around 10^7–10^{10} particles/L with an average diameter of 128 nm [4] which result in a surface area of $5.22*10^{-4}$ m^2/L.

The effect of the presence of particles on nucleation and subsequent growth was addressed by many researchers [5–12], where it was claimed that active impurities, e.g. macro-molecules, organic compounds and metallic ions, may have growth suppression effects on precipitated salts depending on the size, shape, orientation, and molecular size of the impurity [5,11,12]. On the contrary, it was also reported that the presence of particles may affect the mechanism of nucleation of a particular scalant due to the generation of extra nucleation sites associated with the settling of these particles [10,13]. Thompson, 2003 [14] claimed that impurities in the solution induce their effects by interacting with crystal faces during growth; some impurities can completely suppress growth, some enhance growth, while others act selectively or to varying degrees on each crystal face, consequently modifying the crystal morphology [14]. On the contrary, Snoeyink and Jenkins, 1980 [15] demonstrated a negative effect of particles on slightly supersaturated solutions with respect to CaCO$_3$, where these solutions show an infinite degree of stability until fine foreign particles were added. The resultant solution performance in such cases was very similar to what is found if supersaturation was increased [15].

Scaling is considered a continuous hazard in the design and operation of SWRO systems. Calcium carbonate, as the most abundant scalant in SWRO, is commonly assumed to precipitate immediately when its solubility is surpassed. The supersaturation of a solution with regard to calcium carbonate can be calculated using different indices. The most commonly used indices are the Stiff & Davis stability index (S&DSI); Saturation Index (SI) and Saturation ratio (S$_a$) [16–23]. The S&DSI approach is based on correcting the values of the solubility product and second acidity constant for salinity and temperature based on experimental data [22].

$$S\&DSI = pH_c - pH_s \tag{1}$$

$$S\&DSI = pH_c - (pCa + pAlk + k) \tag{2}$$

and

$$k = pK_2 - pK_{sp} \tag{3}$$

When it comes to practice, supersaturated solutions normally exhibit a period of stability after which precipitation takes place [21]. This period of stability is defined as the induction time, and is the time elapsed between the creation of supersaturation and the first appearance of a new phase [21]. Induction time is commonly measured by following the change in either the concentration of one of the crystal ions, pH, conductivity or turbidity over time [24].

Experimentally, it is very difficult to determine the formation of the first nuclei, and consequently, a part of the induction time may also include growth to a detectable size.

The induction time was reported to be affected by the stirring speed applied during the reaction, and was reported to decrease with increasing solution supersaturation and increase as the applied mixing speed increased (300 to 700 rpm) [21,25,26]. This relation may be attributed to the method of measuring induction time and whether the nucleation mechanism was homogenous and heterogeneous [27,28], as homogenous nucleation was reported not to be affected by changing the mixing speed [29]. Unlike its effect on nucleation, their growth experiments, reported that stirring speeds of 300 to 800 rpm had no effect on crystal growth [27,28].

For the purposes of this research it is assumed that the nucleation time is much greater than the time required for growth of crystal nuclei to a detectable size [30]. Thus, induction time can be assumed to be inversely proportional to the rate of nucleation, $t_{ind} \propto J^{-1}$ [21].

$$t_{ind} \propto J^{-1} \tag{4}$$

Where the steady state nucleation rate can be expressed in

$$J_s = \Omega \exp\left[-\frac{\beta \cdot V_m^2 \cdot \gamma^{s^3} \cdot f(0)}{v^2 \cdot (kT)^3 \cdot (\ln S_a)^2} \right] \tag{5}$$

In equation (5) an arbitrary factor ($f(\theta)$) determines the nucleation mechanism. Homogeneous nucleation is recognized by $f(\theta) = 1$ while for heterogeneous nucleation $f(\theta) < 1$. Values as low as 0.01 were reported [21].
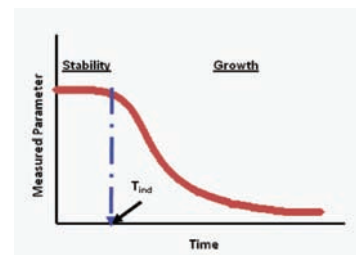

Fig. 1. Schematic diagram showing the experimental detection of induction time.

Based on equations (4) and (5)

$$\log t_{ind} = \frac{B}{T^3 (\log S_a)^2} - A \qquad (6)$$

Based on nucleation theory, homogenous and heterogeneous nucleation mechanisms are basically differentiated by the description of nucleus formation. Nucleation is referred to as homogeneous nucleation when the formation of a solid phase is not influenced by presence of any solid phase, while in heterogeneous nucleation, the formation of new solid phase particles is catalyzed by the presence of a foreign solid phase. When nucleation occurs, growth of a solid phase is then initiated by the presence of the solid phase already formed [21]. The solid phases inside a SWRO module can be particles present in the feed water or the membrane surface itself. In literature, homogenous and heterogeneous nucleation are differentiated by the slope of the relation between Log t_{ind} and Log S_a^{-2} shown in equation (6) [6,11,12,31]. The change in slope is related to the geometrical shape β in equation (5) which represents different crystallization habits at different ranges of supersaturation. For $CaCO_3$, this boundary saturation ratio (S_a) at which β changes ranges between 20 [12] to 100 [31].

2. Materials

The experimental setup shown in Figure 2 was built to measure the induction time using a highly sensitive on-line pH meter (Eutech pH 6000) with an accuracy of 0.001 pH units. The pH meter is connected on-line for continuous measurement of pH with time. The pH probe was fitted in the top of the air-tight double jacketed glass reactor with a volume of 3 liters (Applikon), and equipped with a double paddled shaft mechanical stirrer. The mixing rate can be varied from 0 to 1200 rpm using an electronic controller (Applikon) linked to the mixing motor. The reactor can be filled either mechanically using a diaphragm pump with average filling speed of 4 L/min or manually. After each experiment cleaning employing 0.2 molar HCl or HNO_3 to dissolve any crystals formed was performed for 30 min with a flow of 0.15 L/min, and then flushed with demineralized water for 15 minutes with a flow rate of 3 L/min before the next experiment.

2.1. Synthetic seawater concentrate preparation

The ultra-pure water system is shown in figure 3. Tap water is delivered as the raw water source where it passes through a series of treatment steps to decrease the organic and inorganic particle content in the feed water. The product water had a conductivity and total organic carbon (TOC) 0.8 µS/cm and 3 µg/L, respectively. The TOC was measured using TOC analyzer with detection limit of 0.5 µg/L.

The synthetic seawater concentrate used in the experiments was prepared in stages. First, $NaHCO_3$ was prepared by dissolving 0.81 g/L of $NaHCO_3$ salt (Pro-analysis shown in Table 1) in ultra-pure water. Second,
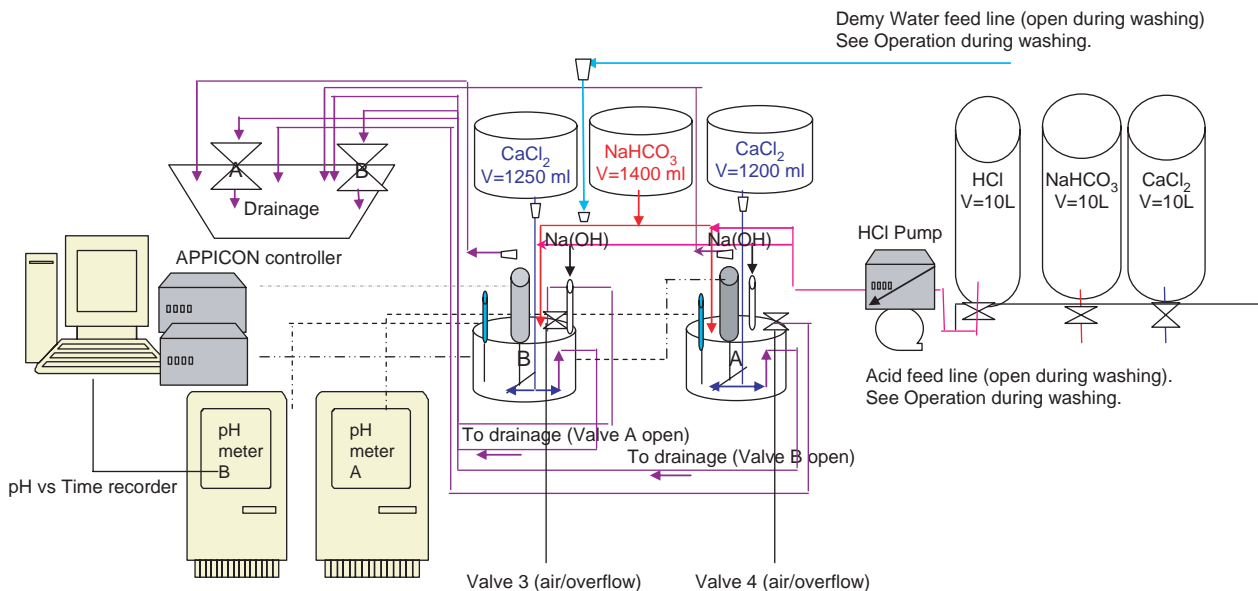

Fig. 2. Schematic general view of the system used during the induction time experiments.
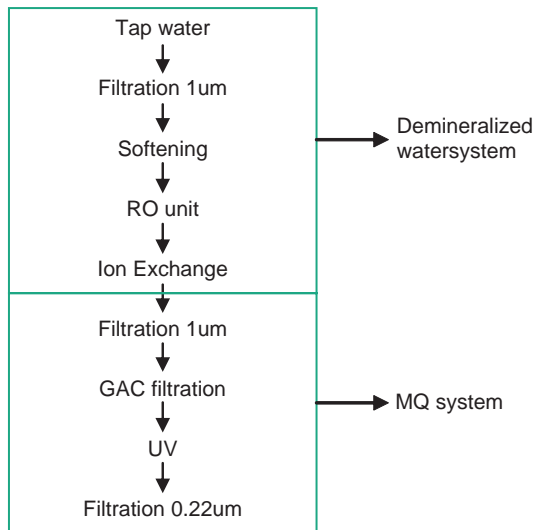
Tap water

↓

Filtration 1um

↓

Softening

↓

RO unit

↓

Ion Exchange

→ Demineralized watersystem

↓

Filtration 1um

↓

GAC filtration

↓

UV

↓

Filtration 0.22um

→ MQ system

Fig. 3. Laboratory Ultra-pure water preparation system.

Table 1
Salt reagents used in experimental synthetic seawater concentrate preparation.

Reagent	Form	Supplier	Purity
NaCl	Salt	J.T. Baker	99.5–99.9 %
$CaCl_2\ 2H_2O$	Salt	MERCK	99.9
$NaHCO_3$	Salt	MERCK	99.9

$CaCl_2\ 2H_2O$ solution was prepared by dissolving 5.25g/L of $CaCl_2\ 2H_2O$. Finally, 17.93 g/L of NaCl salt was dissolved in the previously prepared $CaCl_2\ 2H_2O$ solution to adjust the ionic strength value (1.62 mole/L) of the prepared synthetic concentrate to compensate for the absence of other ions present in real sea water concentrates.

To insure complete dissolutions of reagents, the salt was added to the ultra-pure water in a measuring flask. The flask was then closed and shaken manually for 2 minutes after which 2 hours of solution mixing took place on a magnetic stirrer. Mixing was performed at an average speed of 400 rpm and at room temperature of 20ºC.

The induction time experiments were initiated by adding the $NaHCO_3$ solution into the reactor followed by the NaOH solution for pH correction. Finally the $CaCl_2\ 2H_2O$ + NaCl solution was added with a rate of 0.2 L/min while maintaining a mixing speed of 150 rpm to ensure proper mixing and to prevent the formation of local saturation zones. The addition was performed through fine nozzles located 3 cm from the reactor's bottom to ensure proper distribution of the solution when added. The two reacting solutions were added on a 1:1 volume basis. The resultant synthetic solution is

Table 2
The ionic composition of the experimental synthetic seawater concentrates equivalent to 50% recovery using Gulf of Oman water.

Ions		Experimental solution
Calcium	mg/L	948
Bicarbonate	mg/L	293
Sodium	mg/L	35,382
Chloride	mg/L	56,071
Ionic Strength	Mole/L	1.61

equivalent to 50% recovery SWRO concentrate using the Gulf of Oman as the feed water (Table 2).

3. Methods

The procedure used to study the effect of particles on $CaCO_3$ nucleation comprised of three different experiments,

1. removal of particles in synthetic concentrate by filtration,
2. addition of foreign particles,
3. effect of mixing on the experimental results.

3.1. The effect of particles in synthetic seawater on induction time

Prior to the start of the induction time experiment, the prepared solutions were first filtered separately through either a 0.2 μm; 01 μm or 100kDa (≈0.03 μm), polyethersulphone (PES) membrane (Millipore) with a diameter of 76 mm. Before use, the filters were flushed and then soaked for 1 day in a clean, completely filled with ultra-pure water and sealed plastic cup. Filtration was performed under pressure using an Amicon stainless steel stirred cell at a pressure of 3 bars.

The pH was monitored over a period of at least 1000 minutes and induction time was defined as the time corresponding to a pH drop of 0.03 pH units. This decrease in pH was equivalent to 0.3 mg/L of precipitated $CaCO_3$. The pH of the synthetic concentrate was varied between 7.8 and 8.6 to simulate different levels of supersaturation using 0.2 M NaOH prepared from pure salt (99.99% MERCK) and dissolved in ultra-pure water. The Stiff and Davis saturation index was calculated for each experiment, and the S&DSI vs. induction time was plotted for each test independently.

3.2. Effect of particles addition

The number of particles in the synthetic seawater water was increased by adding inert glass nano-particles

Table 3
Surface area after the addition of 20–30 nm glass beads in the experimental synthetic seawater concentrates.

	Units	Particle addition to synthetic seawater		
		1 ml	0.5 ml	0.1 ml
No. of particles	Particle/L	6.4E+13	8E + 12	6.4E + 10
Area/L	m²/L	0.042	0.005	4.19E − 05
Area reactor/L	m²/L	0.034		
Area other parts/L	m²/L	0.0112		
Area particles/ Area glass	%	123.1	15.4	0.12
Area particles/ Area total	%	92.6	11.6	0.09

with a diameter ranging from 20–30 nm. The particles were introduced into the reactor as a suspension (48% water content supplied by BaseClear). The particles were injected in 3 volumes of either 0.1; 0.5 or 1 ml of suspension producing a particle content of 6.4×10^{-10}; 8×10^{12} or 6.4×10^{13} particle/L, respectively. These glass particles produced an extra surface area for nucleation equal to 4.2×10^{-5}; 0.005 or 0.042 m²/L. Taking into consideration the surface area of the glass reactor walls, mixer shaft, mixing paddle and reactor (metal) cover in contact with the solution (as shown in Table 3), the increase in surface area is equivalent to 0.09%; 11.6% and 92.6% for the 0.1; 0.5 and 1 mL doses, respectively.

The glass particles were added after adding the $NaHCO_3$ solution and mixing was maintained at 150 rpm to insure a proper distribution in the solution. The addition of NaOH and $CaCl_2.2H_2O$+NaCl solutions followed the same procedure described in the synthetic water preparation. Three different levels of saturation were tested namely, S&DSI = 0.77; 0.62 and 0.55 corresponding to initial pH of 8.15; 8.0 and 7.93 respectively.

3.3. Mixing effect

The mixing rate was varied to determine the effect of diffusion on induction time. Three different mixing speeds namely 10; 50 and 300 rpm were tested and compared to results obtained at 150 rpm.

4. Results and discussion

4.1. The effect of particles in synthetic seawater on induction time

Figure 4 shows a sample pH measurement over time for synthetic seawater concentrates pre-filtered through 100kDa (≈0.03 µm) filters. The initial S&DSI was 0.85, and the induction time based on the developed method was estimated to be 25 minutes.

Experiments were performed with synthetic seawater filtered through 0.2 µm; 0.1 µm and 100 kDa (≈0.03 µm) filters. The results presented in Table 4 and Fig. 5, showed

that there is no pronounced effect of filtration on the induction time. This may be attributed to the fact that the ultra-pure water and pro-analysis chemicals used in the preparation of our synthetic seawater resulted in more or less particle free synthetic concentrates or that particles greater than 100 kDa (≈0.03 µm) have a minor effect on the measured induction time. The logarithmic relation between the initial pH and the corresponding induction time agreed with what was previously reported by Waly et al, 2009 [23]. The correlation factor (R^2) for the graph is 0.93; 0.94; 0.92 and 0.94 for unfiltered; 0.2 µm; 0.1 µm and 100 kDa (≈0.03 µm) filters respectively.

In Figure 6, a single logarithmic line appeared to fit all experimental data with a correlation factor of 0.95 and the produced relation suggests that immediate precipitation will not occur except when the solution pH is increased to ca. 9.08.

The relation between the induction time and the S&DSI (Fig. 7) showed that the induction time was greater than 750 min at S&DSI = 0.12 (pH =7.51). This induction period is 100 times shorter (6–7min) at the highest supersaturation level applied of S&DSI ≈ 1.2 (pH = 8.67).
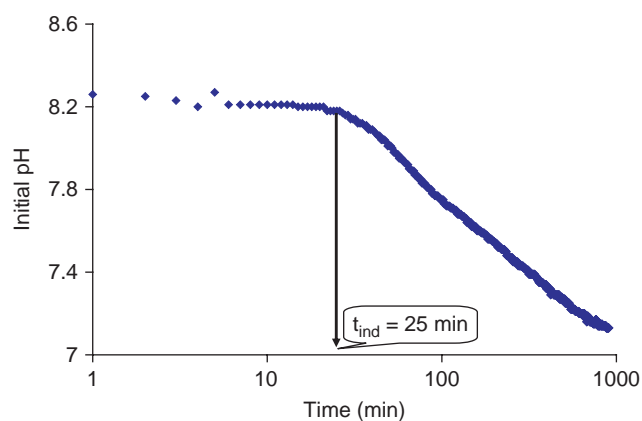

Fig. 4. Initial pH vs. Time (minutes) for synthetic SWRO concentrates (recovery 50%) at mixing speed of 150 rpm and temperature of 20ºC.

Table 4
Synthetic concentrate pH and corresponding Stiff and Davis saturation Index value.

Unfiltered			0.2 μm filtered			0.1 μm filtered			100KDa (≈0.03 μm) filtered		
pH	t_{ind} (min)	S&DSI	pH	t_{ind} (min)	S&DSI	pH	t_{ind} (min)	S&DSI	pH	t_{ind} (min)	S&DSI
7.91	101	0.47	7.83	181	0.39	7.51	778	0.07	7.56	554	0.12
8.20	55	0.76	8.20	44	0.76	7.92	114	0.48	7.82	168	0.38
8.23	41	0.79	8.25	28	0.81	8.09	49	0.65	8.09	60	0.65
8.27	20	0.83	8.31	21	0.87	8.25	68	0.81	8.25	24	0.81
8.34	19	0.90	8.41	20	0.97	8.34	34	0.90	8.52	18	1.08
8.52	11	1.08	8.43	9	0.99	8.41	22	0.97	8.54	10	1.10
8.64	4	1.20	–	–	–	8.53	13	1.09	8.60	13	1.16
–	–	–	–	–	–	8.62	7	1.18	–	–	–
–	–	–	–	–	–	8.67	7	1.23	–	–	–

4.2. Effect of particle addition on induction time

Immediate precipitation was observed when the solution was subjected to a suspension of high surface area glass particles (0.042 m²/L) (Fig. 8). Immediately, visual turbidity and a rapid drop in pH (from initial pH of 8.15 till 7.4) was observed after adding particles (1 mL) and an induction time could not be practically measured (less than 1 min). The pH at which the induction time was instantaneous was (8.15) and is much lower than the value suggested earlier (Fig. 6) of 9.08. In the case of a particle concentration of 8×10^{12} /L (0.005 m²/L), the induction time was 59 min and 78 min for an
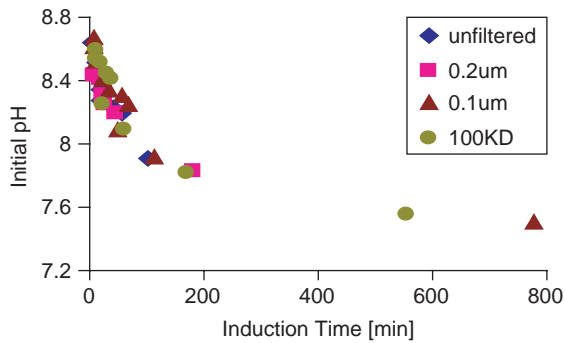

Fig. 5. Effect of filter pore size on induction time of synthetic SWRO concentrate at a mixing speed of 150 rpm and temperature of 20°C.

Fig. 7. Induction time (minutes) vs. Stiff & Davis stability index for synthetic SWRO concentrates (recovery 50%) with all filtered and unfiltered experimental data (mixing speed of 150 rpm and temperature of 20°C).

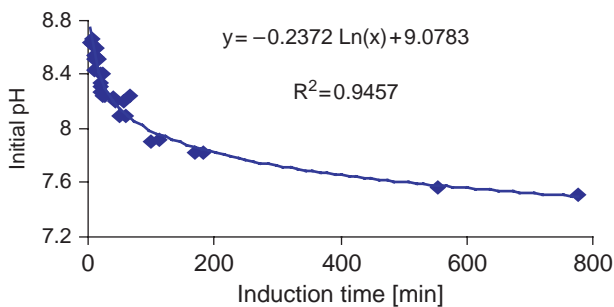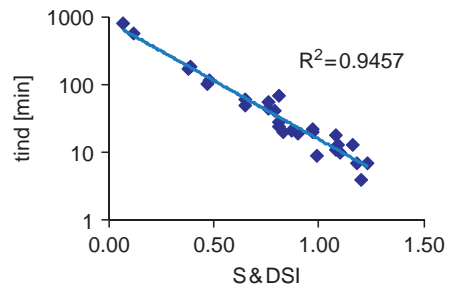$$y = -0.2372 \, Ln(x) + 9.0783$$

$$R^2 = 0.9457$$

Fig. 6. The relation between initial pH and induction time for all data points for synthetic SWRO concentrate at a mixing speed of 150 rpm and temperature of 20°C.
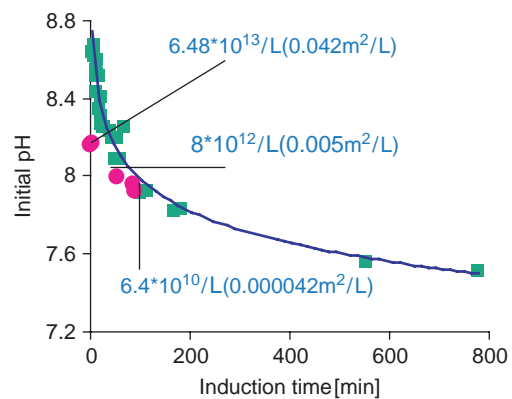
Fig. 8. Induction time as a function of initial pH at various doses of glass beads of 6.48×10^{13}; 8×10^{12} and 6.4×10^{10} particle/L compared to the data obtained with no particle addition (solid line) for synthetic SWRO concentrates of 50% recovery at mixing speed of 150 rpm and 20°C.

Table 5
Calculation of free volume in an 8" SWRO membrane module.

| Parameter	Value
Membrane surface area	32–38 m² (average = 35 m²)
Thickness of spacer	0.52 mm
Membrane diameter	0.2 m
Length of the membrane module	1 m
Volume between the two membrane sheets	35m × 0.52 × 10⁻³m × 1m = 0.0182 m³

Fig. 9. Induction time as a function of initial pH at mixing speeds of 300; 50 and 10rpm (red circles). Data obtained at 150rpm (green squares fitted with blue line) are also plotted for comparison (blue line).

initial pH of 8 and 7.93, respectively. When compared to induction times measured for 'particle free' (filtered) solution, these results are 30% lower than the expected values of 90 and 120 minutes. A visible observation of the glass reactor after the experiment showed that the reactors were scratched probably as a result of glass bead addition in combination with vigorous stirring. Scratching of the reactor wall may have resulted in the creation of new (fresh) particles that may stimulate the nucleation process [15].

In real SWRO plants, the surface area of the membrane in direct contact with water inside a module is nearly 1.9 m²/L. The calculations are based on membrane surface area of 32–38m² and a spacer thickness of 0.52 mm for an 8-inch membrane with 1 m length. The total free volume occupied by the feed water is nearly 18.2 L. The surface area of the RO membrane (1.9 m²/L) is more than 3600 times greater than the surface area of particles in real seawater (5.22 × 10⁻⁴ m²/L) as suggested [4]. This may suggest that membrane scaling of SWRO modules is highly likely to be influenced by the membrane surface in direct contact with the concentrate, rather than particles present in the feed water.

4.3. Effect of mixing speed on induction time

The mixing speed used in the experiments was varied between 10; 50 and 300 rpm and results of induction time were compared with results employing a mixing speed of 150 rpm (green squares in the log relation plotted in Fig. 9). The results shown in Fig. 9 suggest that the mixing speed had almost no effect on the induction time in the tested range of mixing speed and saturation. These results agree with those documented [27,28] which conclude that the induction time was independent of the mixing rates applied. Others confirmed the effect of mixing on induction time [21,32,33]. This effect was minimum at high supersaturation ratios (mainly in the homogenous range) [29]. This may suggest that the supersaturation values tested for the effect of mixing (S_a = 20–40) lies in the homogenous nucleation zone rather than the heterogeneous zone. However, further research is needed to prove this hypothesis.
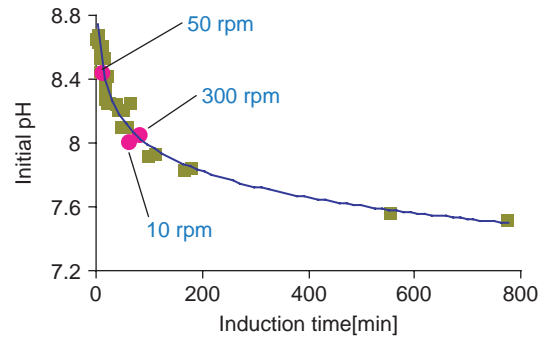
4.4. Mechanism of nucleation

The experimental results of this study were compared to the classification developed by Sohnel and Mullin, 1982 [12] to identify the zones of homogenous and heterogeneous nucleation for $CaCO_3$. According to [12], if Log (t_{ind}) is plotted against $Log^{-2} S_a$ for a wide range of saturations, two slopes can be identified (Fig. 10). The range of saturation corresponding to the steeper slope was assigned the homogenous zone of nucleation while the range of supersaturation corresponding to the lower slope represents the heterogeneous zone. In between the two slopes an intermediate zone exists, where a transition between the two nucleation mechanisms takes place [12].

Induction time values measured in this study were considerably longer than that reported [12], but agreed with other researchers results at the same supersaturation ratio [34–36]. For example, for a Log $(S_a)^{-2}$ of 0.5 corresponding to an S&DSI = 0.81, Sohnel and Mullin, 1982 [12] reported 0.1 sec induction time. However, in this study, the measured induction time at the same supersaturation was 44–55 minutes. In general the experimental
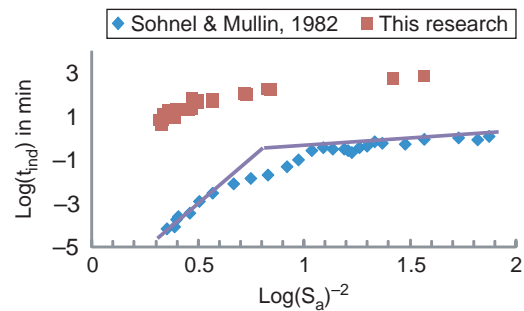

Fig. 10. The relation between Log t_{ind} & Log $(S_a)^{-2}$ for this research compared it with Sohnel & Mullin, 1982 [12].

Table 6
Synthetic concentrate pH and corresponding Saturation index (SI) and saturation ratio (S_a) calculations by PhreeqC using Pitzer activity coefficients and calcite solubility.

Initial pH	t_{ind}[min]	Log t	SI	S_a	(Log S_a)$^{-2}$
7.91	101	2.00	1.17	14.79	0.731
8.20	55	1.74	1.42	26.30	0.496
8.23	41	1.61	1.45	28.18	0.476
8.27	20	1.30	1.48	30.20	0.457
8.34	19	1.28	1.53	33.88	0.427
8.52	11	1.04	1.67	46.77	0.359
8.64	4	0.60	1.75	56.23	0.327
7.83	181	2.26	1.10	12.59	0.826
8.20	44	1.64	1.42	26.30	0.496
8.25	28	1.45	1.46	28.84	0.469
8.31	21	1.32	1.51	32.36	0.439
8.41	20	1.30	1.59	38.90	0.396
8.43	9	0.95	1.60	39.81	0.391
7.51	778	2.89	0.80	6.31	1.563
7.92	114	2.06	1.18	15.14	0.718
8.09	49	1.69	1.33	21.38	0.565
8.25	68	1.83	1.46	28.84	0.469
8.41	22	1.34	1.59	38.90	0.396
8.53	13	1.11	1.67	46.77	0.359
8.62	7	0.85	1.73	53.70	0.334
8.67	7	0.85	1.77	58.88	0.319
7.56	554	2.74	0.84	6.92	1.417
7.82	168	2.23	1.09	12.30	0.842
8.09	60	1.78	1.33	21.38	0.565
8.25	24	1.38	1.46	28.84	0.469
8.52	18	1.26	1.67	46.77	0.359
8.54	10	1.00	1.68	47.86	0.354
8.60	13	1.11	1.72	52.48	0.338

induction times measured in this research (Table 6) were a factor of 1000 to 10000 greater than that measured by [12]. The experimental data generated in this study were plotted in Figure 10 , and it can be seen that most of our data lie in the homogenous and the transition nucleation zones as defined by [12].

When (Log^{-2} S_a) was calculated for the mixing speed experiments (Fig. 9), results showed values of 0.67, 0.61 and 0.39 for mixing speeds of 10, 300 and 50 rpm, respectively. These values appear to lie in the homogenous range as defined earlier [12]. The minor effect of mixing on induction time may be explained by the fact that homogenous nucleation dominated as it was reported that the effect of mixing is minor when homogenous nucleation is the governing mechanism. On the contrary, the effect on the induction time is expected to be greater when heterogeneous nucleation predominates [21,27, 8,32,33].

5. Conclusions

Supersaturated SWRO concentrate (recovery of 50%) was produced by dissolving pure salts (99.9%) in ultra pure water to avoid the presence of foreign particles in the supersaturated solution. In addition the supersaturated solutions were pre-filtered with either 0.2 μm; 0.1 μm and 100 kDa (0.03 μm) filters to remove any particles present in the solution. No effect of pre-filtration with 0.2 μm; 0.1 μm and 100 kDa (0.03 μm) was observed on induction time for synthetic SWRO case with initial S&DSI of 0.12 to 1.28. A possible explanation for this result may be that particles smaller than 0.03 μm affect induction time. However more research is required to verify this hypothesis.

The induction time for $CaCO_3$ in synthetic seawater concentrate was not affected by the range of mixing rates tested in this study (10–300 rpm). For example, at 50 rpm the induction time was 14 min compared to 15 min in case of 150 rpm. According to the definition of how to differentiate between homogenous and heterogeneous nucleation mechanisms proposed by Sohnel and Mullin, 1982 [12], most of the experimental data produced in this study lies in the homogenous and intermediate zones. This may explain the minor effect of mixing on the induction time.

Nomenclature

A	Function of Pre-exponential factor (s^{-1}m^{-3})
A^*	Deby Huckel constant (L$^{2/3}$mol$^{-1/2}$)
a_c	Activity
A_f	Free area for precipitation at given particle size (m^2)
Alk	Alkalinity of solution (mole/L)
B	Constant expressed in equation 1.7 (L$^{3/2}$ mol$^{-1/2}$nm^{-1})
$f(\theta)$	Factor differentiating heterogeneous and homogenous nucleation
I	the ionic strength (mol/L)
IAP	ionic activity product (mol^2/L^2)
J	Nucleation rate (nuclei/min/cm^3)
Js	Steady state nucleation rate (nuclei/min/cm^3)
k	Boltzmann constant (J/K)
K_{sp}	Solubility product (mole^2/L^2)
K_{a2}	Second acidity constant (mole/L)
pH_c	Concentrate pH
pH_s	Equilibrium pH
SI	Supersaturation Index
S_a	Supersaturation ratio
T	Absolute temperature in Kelvin

t_{ind}	Induction time in minutes unless mentioned otherwise (min)
v	Number of ions into which a molecule dissociate
V_m	Molecular volume (cm^3/mole)

Symbols

β	Geometric factor
γ_+	Cation activity coefficient
γ_-	Anion activity coefficient
γ^s	Surface energy (J/m^2)
Ω	Pre-exponential factor in the nucleation rate equation ($s^{-1}m^{-3}$)

References

[1] D.E. Potts, R.C. Ahlert and S.S. Wang, A critical review of fouling of reverse osmosis membranes, Desalination, 36 (1981) 235–264.

[2] S.G. Yiantsios and A.J. Karabelas, An assessment of Silt density index based on RO membrane colloidal fouling experiments with iron oxide particles, Desalination, 151 (2002) 229–238.

[3] S.C.J.M.V. Hoof, J.G. Minnery and B. Mack, Performing a membrane autopsy, Desalination Water Reuse, 11 (2002) 40–46.

[4] K. Park, et al., Measurement of size and number of suspended and dissolved nonoparticles in water for evaluation of colloidal fouling in RO membranes, Desalination, 238 (2009) 78–89.

[5] N. Kubota and J.W. Mullin, A kinetic model for crystal growth from aqueous solution in the presence of impurity, Journal of Crystal Growth, 152 (1995) 203–208.

[6] E. Abdel-Aal, M. Rashad and H. El-Shall, Crystallization of calcium sulfate dihydrate at different supersaturation ratios and different free sulfate concentrations, Cryst. Res. Technol., 39 (2004) 313–321.

[7] P. Zuddas and A. Mucci, Kinetics of calcite precipitation from seawater: II the influence of the ionic strength, Geochimica et Cosmochimica Acta, 62 (1998) 757–766.

[8] T. Chen, A. Neville and M. Yuan, Assessing the effect of Mg2+ on CaCO3 scale formation–bulk precipitation and surface deposition, Journal of Crystal Growth, 2005. 275: p. 1341–1347.

[9] D.K. Gledhill and J.W. Morse, Calcite dissolution kinetics in Na–Ca–Mg–Cl brines, Geochimica et Cosmochimica Acta, 70 (2006) 5802–5813.

[10] D.K. Gledhill and J.W. Morse, Calcite solubility in Na–Ca–Mg–Cl brines, Chemical Geology, 233 (2006) 249–256.

[11] E. Kirkova and M. Djarova, On the Kinetics of Crystallization of Zinc Oxalate Dihydrate by Precipitation Industrial Crystallization, 78 (1979) 81–89.

[12] O. Sohnel and J.W. Mullin, Precipitation of calcium carbonate, Journal of Crystal Growth, 60 (1982) 239–250.

[13] B. Bansal, H. Muller-Steinhagen and X.D. Chen, Effect of suspended particles on crystallization fouling in plate heat exchangers, ASME, 119 (1997) 568–574.

[14] C. Thompson, Investigating the fundamentals of drug crystal growth using atomic force microscope, The University of Nottingham, 2003.

[15] V. Snoeyink and D. Jenkins, Water Chemistry, New York: John Wiley & Sons, 1980.

[16] ASTM, Calculation and Adjustment of the Stiff and Davis Stability Index for Reverse Osmosis, ASTM International: West Conshohocken, PA, United States, 2001.

[17] H. Elfil and H. Roques, Role of hydrate phases of calcium carbonate on the scaling phenomenon, Desalination, 137 (2001) 177–186.

[18] S. El-Manharawy and A. Hafez, Water type and guidelines for RO system design, Desalination, 139(1–3) (2001) 97–113.

[19] J. Schippers, Membrane filtration—Reverse Osmosis, Nanofiltration & Electrodialysis, Delft: UNESCO-IHE, 2003.

[20] R. Sheikholeslami, Assessment of the scaling potential for sparingly soluble salts in RO and NF units, Desalination, 167 (2004) 247–256.

[21] O. Sohneland J. Garside, Precipitation basis principals and industrial applications, Oxford: Butterworth-Heinemann, 1992.

[22] H.A. Stiff and L.E. Davis, A method for predicting the tendency of oil field waters to deposit calcium carbonate, Petroleum transactions, (1952) 213–216.

[23] T. Waly, et al., Will calcium carbonate really scale in seawater reverse osmosis? Desalination and water treatment, 5 (2009) 252–256.

[24] S. Boerlage, Scaling and particulate fouling in membrane filtration system, in Sanitary Engineering, IHE: Delft, 2002.

[25] J.W. Mullin and S. Zacek, The precipitation of potassium aluminium sulphate from aqueous solution, Journal of Crystal Growth, 53 (1981) 515–518.

[26] S. Yu-zhu, et al., Seeded Induction Period and Secondary Nucleation of Lithium Carbonate, The Chinese Journal of Process Engineering, 9(4) (2009) 652–660.

[27] D. Trainer, A study of calcium carbonate crystal growth in the present of a calcium complexing agent, The Institute of Paper Chemistry: Wisconsin, 1981.

[28] H.N.S. Wiechers, P. Sturrock and G.V.R. Morais, Calcium carbonate crystallization kinetics, Water Res., 9 (1975) 835–845.

[29] O. Sohnel and J.W. Mullin, Influence of mixing on batch precipitation, Crystal Research and Technology, 22(10) (1987) 1235–1240.

[30] O. Sohnel, Electrolyte crystal-aqueous solution interfacial tensions from crystallization data, Journal of Crystal Growth, 57 (1982) 101–108.

[31] A.G.Walton, In dispersion of powders in liquids, 2nd ed., London: Appl. Sci. Publ., 1973.

[32] R. Kuboi, et al., Mixing Effects in Double-Jet and Single-Jet Precipitation. in World Congress III of Chemical Engineering,Tokyo, 1986.

[33] R. Mohanty et al., Characterizing the product crystals from a mixing tee process, AIChE journal, 34(12) (1988) 2063–2068.

[34] F.H. Butt, F. Rahman and U. Baduruthamal, Hollow fine fiber vs. spiral-wound reverse osmosis desalination membranes Part 2: Membrane autopsy, Desalination, 109 (1997) 83–94.

[35] A. Hannachi et al. A new index for scaling assessment. in IDA World Congress-Maspalomas, Gran Canaria.

[36] P. Koutsoukos and C. Kontoyannis, Precipitation of calcium carbonate in aqueous solutions. J. Chem. Soc., Faraday Trans. I, 80 (1984) 1181–1192.